



IAEA

INTERNATIONAL ATOMIC ENERGY AGENCY

21st IAEA Fusion Energy Conference

Chengdu, China, 16-21 October 2006

IAEA-CN-149 / EX / 8-5Ra

Microturbulence in Magnetic Fusion Devices: New Insights from Gyrokinetic Simulation and Theory

F. Jenko¹, C. Angioni¹, T. Dannert¹, F. Merz¹, A.G. Peeters¹, P. Xanthopoulos²

¹Max-Planck-Institut für Plasmaphysik, EURATOM Association, 85748 Garching, Germany

²Max-Planck-Institut für Plasmaphysik, EURATOM Association, 17491 Greifswald, Germany

This is a preprint of a paper intended for presentation at a scientific meeting. Because of the provisional nature of its content and since changes of substance or detail may have to be made before publication, the preprint is made available on the understanding that it will not be cited in the literature or in any way be reproduced in its present form. The views expressed and the statements made remain the responsibility of the named author(s); the views do not necessarily reflect those of the government of the designating Member State(s) or of the designating organization(s). In particular, neither the IAEA nor any other organization or body sponsoring this meeting can be held responsible for any material reproduced in this preprint.

Microturbulence in Magnetic Fusion Devices: New Insights from Gyrokinetic Simulation and Theory

F. Jenko¹, C. Angioni¹, T. Dannert¹, F. Merz¹, A.G. Peeters¹, P. Xanthopoulos²

¹Max-Planck-Institut für Plasmaphysik, EURATOM Association, 85748 Garching, Germany

²Max-Planck-Institut für Plasmaphysik, EURATOM Association, 17491 Greifswald, Germany
e-mail: jenko@ipp.mpg.de

Abstract By means of simulation results obtained with the gyrokinetic turbulence code GENE and their theoretical interpretation, the physics of microturbulence in both tokamaks and stellarators is studied. In this context, several critical issues in current plasma microturbulence research are addressed: (1) the nature, nonlinear saturation, and parameter dependencies of collisionless trapped electron turbulence, (2) the origin and character of anomalous particle pinch effects, and (3) the similarities and differences of tokamaks and stellarators with respect to microinstabilities and the associated turbulent transport.

1. Introduction

The ultimate goal of gyrokinetic simulation of microturbulence is to be able to quantitatively predict the turbulent transport in magnetic fusion devices. But while gyrokinetic codes are gradually reaching a level of maturity that actually allows for direct comparisons with experiments, our understanding of the underlying physical processes is still quite fragmentary. Therefore reliable large-scale simulations will have to be based on careful studies of various aspects of somewhat reduced systems.

In the present paper, we will address three critical issues in current plasma microturbulence research:

- electron thermal transport by collisionless trapped electron modes in plasmas with dominant electron heating;
- the physics of anomalous particle pinch effects and its impact on the density profile;
- a comparison of the properties of core turbulence in tokamaks and stellarators.

The work presented here is based on the gyrokinetic turbulence code GENE [1,2] which contains fully gyrokinetic ions and electrons (both passing and trapped), dynamical finite β effects associated with magnetic field fluctuations, collision operators for each particle species (involving energy scattering), beam ion species with non-Maxwellian velocity distribution functions, general (tokamak or stellarator) geometry, and equilibrium $\mathbf{E} \times \mathbf{B}$ shear.

Interestingly, it will turn out that many nonlinear simulation results can be understood even quantitatively in terms of a carefully modified quasilinear transport model which will be described below. This raises the hope that – at least under certain conditions – key aspects of turbulent transport can be described reasonably well by such simplified descriptions which can be used for quick and easy analyses of particular experiments. However, one always has to remain cautious and aware of the limits of such attempts. Eventually, all transport models have to be (double-)checked against *ab initio* theory, namely nonlinear gyrokinetics.

The three topics mentioned above will be treated in sections 2-4. In Section 2, we will investigate the basic properties of collisionless trapped electron mode turbulence. With zonal flows playing only a subdominant role in this case, a different nonlinear saturation mechanism is found which can be described in the framework of a test mode approach. Based on these findings, it is possible to construct a quasilinear transport model that is able to capture many features of this kind of turbulence even quantitatively. In Section 3, this same model is then used to explain the occurrence of anomalous particle pinches. A first comparison between tokamaks and the Wendelstein 7-X stellarator is presented in Section 4. Section 5 contains some important conclusions which can be drawn from this work.

2. Electron thermal transport in plasmas with dominant electron heating

Trapped electron modes (TEMs) are considered to be the main driver of anomalous transport in a large number of dedicated experiments with dominant electron heating which have been performed over the past several years.[3–6] [Usually, the ion temperature in these discharges was much lower than the electron temperature such that electron temperature gradient (ETG) modes were found to be linearly stable.] On the basis of GENE simulations, we have performed the first systematic investigation of TEM turbulence from a theoretical point of view (some of these results have been presented in Ref. [2]). Inspired by some of the experiments mentioned above, we use the following physical parameters: $R/L_n = 3$, $R/L_{T_e} = 6$, $R/L_{T_i} = 0$, $\epsilon_t \equiv r/R = 0.16$, $q = 1.4$, $\hat{s} = 0.8$, $T_e/T_i = 3$, and $\beta_e \equiv 4\pi p_{e0}/B_0^2 = 10^{-3}$. For simplicity, the mass ratio has been reduced to $m_i/m_e = 400$. This has relatively little effect on the results (see Ref. [2]) and helps to save computational resources. The numerical parameters are also discussed in Ref. [2] along with some convergence checks.

The nonlinear simulations can be diagnosed in various ways. In Fig. 1, the k_y spectra of the transport fluxes are shown. Here, thick lines indicate negative values, so that the passing electrons are actually transported inwards (up-gradient), in contrast to the trapped electrons which are transported outwards (down-gradient) and which dominate the particle transport. We note that the transport is driven primarily in the range $k_y\rho_s \sim 0.1$ - 0.2 which is way below the position of the fastest growing linear TEM ($k_y\rho_s \sim 0.4$).

A second interesting diagnostics is shown in Fig. 2. Here, we have plotted the probability distribution functions of the cross phases of pairs of fluctuating quantities as a function of k_y . It is obvious that in the transport-dominating range, i.e., for $0.1 < k_y\rho_s < 0.2$, the cross phases are by no means random but rather clearly defined. Moreover, they tend to lie close to the linear values (shown as thick white lines). This means that the dominating nonlinear modes resemble the respective linear microinstabilities.

In order to assess the role of zonal flows, the following test has been performed. We have taken several simulations well into the saturated regime, and then zeroed out all zonal potential components (see Ref. [2]). It turns out that although the system reacts to that change, the statistical properties of the quasisteady state are not significantly affected – at least if one does not operate very closely to the linear threshold in the normalized electron temperature gradient (weak turbulence regime). In particular, the transport levels are practically the same. This is, of course, in stark contrast to adiabatic ion temperature gradient (ITG) turbulence. Here, zeroing out zonal flows results in a drastic increase of the fluctuation amplitudes and radial heat flows. This implies that TEM turbulence and ITG turbulence must be very different with respect to their nonlinear saturation mechanisms.

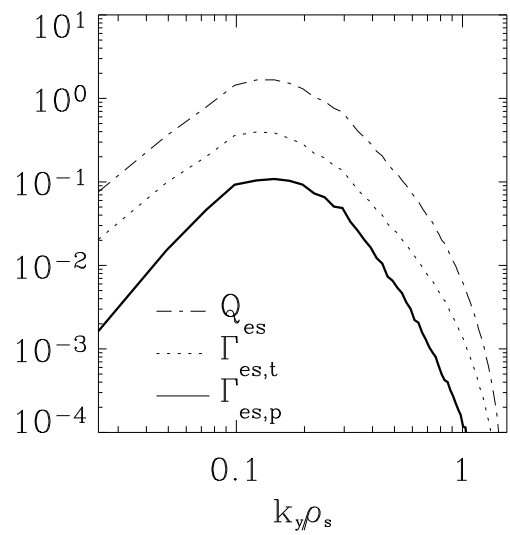


Figure 1: Collisionless TEM turbulence: Transport spectrum in k_y space. Shown are the electrostatic heat flux Q_{es} , the trapped electron flux $\Gamma_{es,t}$ and the passing electron flux $\Gamma_{es,p}$. Thick lines indicate negative values.

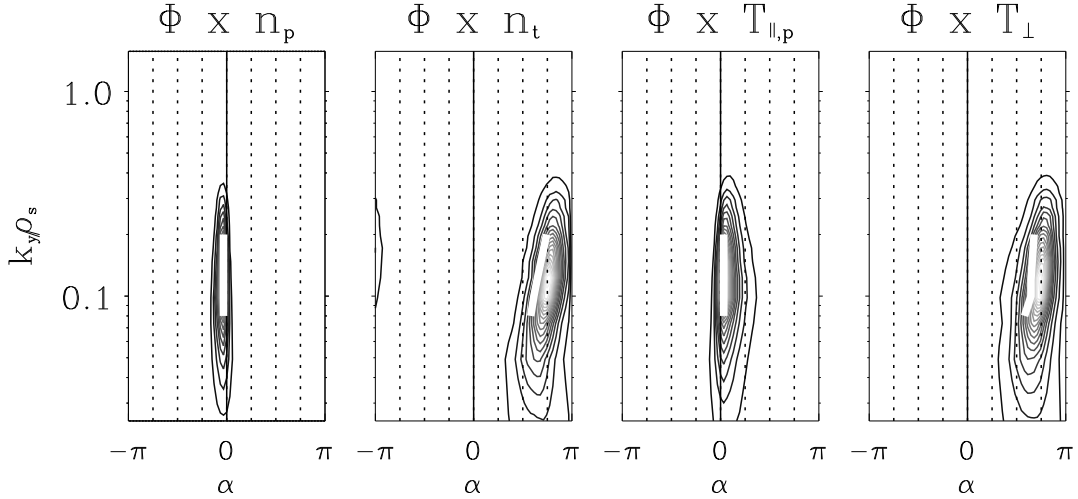


Figure 2: Collisionless TEM turbulence: Phase relations between the electrostatic potential and the passing/trapped electron density as well as the parallel/perpendicular electron temperature. For comparison, the linear results are shown as thick white lines.

This forces us to look for possible saturation mechanisms beyond zonal flow dynamics. As it will turn out, in the context of TEM turbulence, the $\mathbf{E} \times \mathbf{B}$ nonlinearity $\mathbf{v}_E \cdot \nabla \tilde{f}$ is well represented by a diffusion term of the form $D \nabla^2 \tilde{f}$. This is shown in Fig. 3. Here, we plotted the real and imaginary part of the (averaged) ratio between $\mathbf{v}_E \cdot \nabla \tilde{f}$ and \tilde{f} as a function of k_y for $k_x = 0$. While the imaginary part is close to zero, the real part is very close to a parabola. Physically speaking, this means that the long-wavelength modes can be considered as test modes in the presence of small-scale fluctuations which act like a diffusivity. If one solves a modified linear gyrokinetic problem (involving an additional diffusion term) instead of the usual one, one finds that with increasing diffusion coefficient D , the growth rate of a particular mode falls off linearly. Thus, for a critical value of D , the mode becomes marginally stable. We find that the cross phases are only weakly affected, in accord with the above nonlinear results.

All these findings can serve as a basis for a carefully constructed quasilinear transport model. Assuming $k_x = 0$ and $\alpha = 0$, we have

$$\langle k_\perp^2 \rangle = k_y^2 (1 + \hat{s}^2 \langle \theta^2 \rangle) \quad (1)$$

for the average value of k_\perp^2 where θ is an extended, angle-like coordinate in the field-line direction and

$$\langle \theta^2 \rangle \equiv \frac{\int \theta^2 |\phi_{k_y}(\theta)|^2 d\theta}{\int |\phi_{k_y}(\theta)|^2 d\theta}. \quad (2)$$

Here, the weighting is done in terms of the (complex-valued) eigenfunction $\phi_{k_y}(\theta)$ for a given

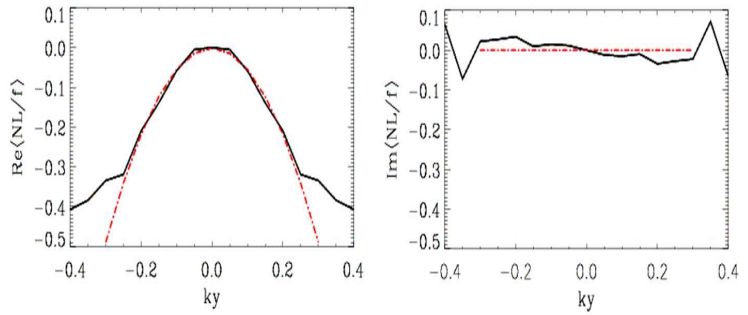


Figure 3: Ratio of the $\mathbf{E} \times \mathbf{B}$ nonlinearity $\mathbf{v}_E \cdot \nabla \tilde{f}$ and the distribution function \tilde{f} as a function of k_y for $k_x = 0$. This shows that the $\mathbf{E} \times \mathbf{B}$ nonlinearity is well represented by a diffusion term of the form $\nabla^2 \tilde{f}$.

set of plasma parameters and a given value of k_y . Consequently, holding all plasma parameters fixed, $\gamma/\langle k_\perp^2 \rangle$ is a function of k_y . Based on these results, one can estimate the electron heat flux Q_e via

$$\frac{Q_e}{n_{e0}T_{e0}/R} = C \max_{k_y} \left[\frac{\gamma}{\langle k_\perp^2 \rangle} \right] \frac{R}{L_{T_e}}, \quad (3)$$

and the ion heat flux Q_i as well as the particle flux Γ via the ratios of the corresponding quasi-linear estimates. The additional factor of R/L_{T_e} mediates between χ_e and Q_e , and the free parameter C is determined such that Q_e agrees with the nonlinear simulation result for some set of base case parameters.

Comparing this transport model with the nonlinear simulations, we find that (see Ref. [2]):

- the nonlinear transport spectra in k_y space are matched nicely by the $\gamma/\langle k_\perp^2 \rangle$ curves as can be seen in Fig. 4;
- the dependence of the transport on the safety factor q is captured well by the transport model (in contrast to standard quasilinear models);
- both approaches show the existence an effective threshold in R/L_{T_e} (for large values of R/L_n) which is not predicted by linear theory.

As will be described next, the above quasi-linear model also allows to predict the particle transport in ITG or TEM turbulence. In particular, the critical values of R/L_n at which the particle transport has its null obtained from this model is in good agreement with the results from nonlinear gyrokinetic simulations.

3. The physics of anomalous particle pinch effects

Experimentally, it is well known that under certain conditions, the particle transport is up-density-gradient. The physics of this particle pinch effect has been investigated with the help of carefully analyzed GENE simulations. It was found that both TEMs and ITG modes are able to produce such a particle pinch – carried, respectively, by passing and trapped electrons. The existence and dominance of either one of these phenomena is shown to be closely linked to the value of the normalized density and temperature gradients. In both scenarios, our refined quasilinear transport model again provides a fairly good description of the nonlinear results.

First, we would like to focus on the following scenario which is typical for most present-day (and future) tokamak experiments: $T_e \sim T_i$ and $R/L_{T_e} \sim R/L_{T_i} > 6$. For concreteness, we choose $T_e/T_i = 1$, $R/L_{T_i} = R/L_{T_e} = 9$, $q = 1.4$, $\hat{s} = 0.8$, $\alpha = 0$, $\epsilon \equiv r/R = 0.16$, $m_i/m_e = 1836$, and $\beta_e = 10^{-4}$ as our base case values. Collisions are neglected. A linear microinstability analysis reveals that for such plasma parameters and small R/L_n , the turbulence tends to be mainly driven by ITG modes. However, increasing R/L_n , we find that the system transitions into a regime which is instead dominated by density gradient driven TEMs. Here, the particle transport is quite large and outward. For illustration, a R/L_n scan is shown in Fig. 5. The fact that for small R/L_n , we have $Q_i \gg Q_e$ while for larger R/L_n , we have $Q_i \sim Q_e$, may be taken as another signature of the regime transition from ITG drive to TEM drive.

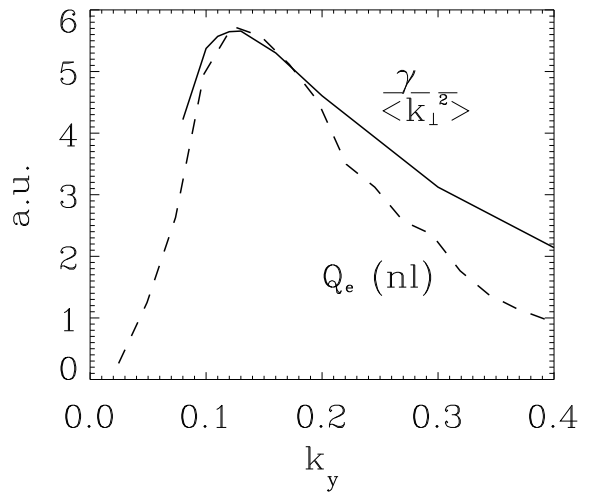


Figure 4: Transport estimate $\gamma/\langle k_\perp^2 \rangle$ as a function of k_y . The k_y spectrum of the electron heat flux obtained from a nonlinear GENE simulation is shown for comparison as a dashed line. Here, the $\gamma/\langle k_\perp^2 \rangle$ curve has been rescaled to match the nonlinear result at its maximum.

From an experimental point of view, the value of R/L_n for which the particle flux vanishes is of particular interest. Provided that the particle source in the plasma core is negligible, it is reasonable to expect that fusion plasmas tend to self-organize into states of marginal particle transport. We thus performed a large number of nonlinear GENE runs to identify the critical R/L_n as a function of the magnetic shear. The result is shown in Fig. 6. For comparison, we also computed the corresponding results from (a) the quasilinear model described above, (b) the widely used quasilinear GLF23 gyro-Landau fluid model [7], and (c) the turbulent equipartition (TEP) theory by Isichenko and co-workers as described in Ref. [8]. While the quasilinear model agrees with the nonlinear results quite nicely, the other two models are only able to capture the general trend. In the case of GLF23, one source of the observed discrepancy is, of course, the difference in the basic equations. But as it turns out, there is yet another, quite subtle point which can also alter the results quite significantly and which is usually overlooked. As is shown in Ref. [9], the sign of the linear phase shifts between the density fluctuations and the electrostatic potential fluctuations is a function of k_y . [Negative values correspond to inward particle transport and vice versa.] Consequently, if the transition point is computed by means of a quasilinear model, the answer will depend on the value of k_y that is chosen. As was discussed already in Section 2, the nonlinear transport spectra typically peak at much smaller values of k_y and move around as the plasma parameters are changed. Since our modified transport model accounts for these effects, it is able to reproduce the nonlinear results quite nicely.

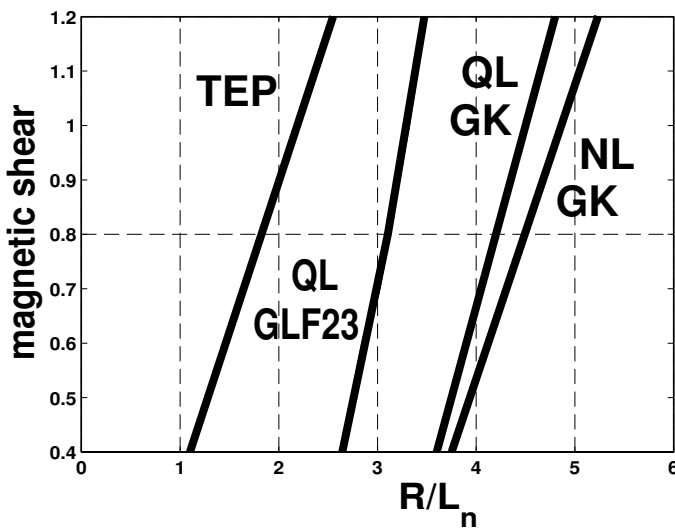


Figure 6: Lines of zero particle flux in the R/L_n - \hat{s} plane for four different models: (a) nonlinear gyrokinetics (NL GK), (b) the quasilinear model (QL GK), (c) GLF23 (QL GLF23), (d) turbulence equipartition theory (TEP).

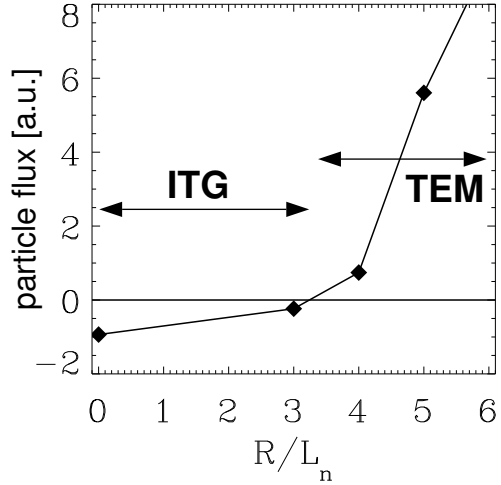


Figure 5: Dependence of the particle flux on R/L_n . For $R/L_n < 3.5$, the turbulence is driven mainly by ITG modes and exhibits a particle pinch. For larger values of R/L_n , the system transitions into a regime which is dominated by density gradient driven TEMs. Here, the particle transport is quite large and outward.

It is also interesting to investigate the role of trapped and passing electrons in pinch physics. Such studies have been reported in Ref. [9]. Here, it was shown, in particular, that both trapped (TEM case) and passing (ITG case) electrons are able to carry a particle pinch. A general prerequisite for the occurrence of a particle pinch is that the 'passive' temperature gradient (R/L_{T_i} in the TEM case and R/L_{T_e} in the ITG case) is sufficiently large. The possibility of a passing electron pinch implies that simple models with bounce-averaged trapped electrons and adiabatic passing electrons will miss this effect.

4. Comparing core turbulence in tokamaks and in the stellarator Wendelstein 7-X

In this section, we present the first gyrokinetic simulations of ion-scale core turbulence in stellarator geometry, highlighting some striking similarities and differences between stellarators and tokamaks.

Advanced stellarators like the Helias configuration Wendelstein 7-X [10] will be used to explore the suitability of the stellarator concept as a basis for future fusion power plants. Unfortunately, little is known at present about the level of turbulent transport to be expected in those devices. In this context, it is important to note that Wendelstein 7-X has been designed such that regions with a large fraction of magnetically trapped particles are characterized by relatively small magnetic curvature and vice versa. Consequently, one expects that TEMs are weaker than in tokamaks and that the impact of trapped electrons on ITG turbulence is strongly reduced.

Our first goal is to test these ideas for various linear microinstabilities. We use a $\beta = 0$ MHD equilibrium for Wendelstein 7-X and start by investigating adiabatic ITG modes, setting $R/L_n = 0$, $T_e/T_i = 1$, and $k_{\perp}\rho_i = 0.3$. The geometric coefficients are computed and used according to the description in Ref. [11]. The relative simplicity of the present case allows for an analytical treatment based on a reduced gyrofluid model (see, e.g., Ref. [12]). This approach successfully describes the linear growth rates for large values of the ion temperature gradient, thus providing an estimate for the ‘effective’ critical gradient $(R/L_{T_i})_{\text{crit}}$ of the toroidal branch.

According to such a simple model, the latter is expected to scale as

$$\gamma \propto \frac{c_s}{\sqrt{RL_{T_i}}} \left[\frac{R/L_{T_i} - (R/L_{T_i})_{\text{crit}}}{R/L_{T_i}} \right] \quad (4)$$

at fixed k_y . This expectation is verified for the W7X case in Fig. 7. Indeed, the fit of the toroidal branch of the linear growth curve to the above expression is excellent. By means of this procedure, it is thus possible to extract the effective threshold for the ion temperature gradient. It is given by $(R/L_{T_i})_{\text{crit}} \approx 9$. Below this value, the toroidal ITG mode transitions into a trapped ion mode as can be inferred from inspection of the amplitude profiles in the parallel spatial direction.

Using exactly the same physical setup, we have performed three nonlinear gyrokinetic simulations for $R/L_{T_i} \in \{12, 15, 18\}$. The time traces for the normalized ion heat fluxes are shown in Fig. 8. Performing time averages over the last 40% of the run time, one obtains $\chi_i [\rho_i^2 v_{ti}/R] = \{0.07, 0.22, 0.40\}$ for each of the respective cases. This demonstrates that the present system exhibits a nonlinear upshift of $(R/L_{T_i})_{\text{crit}}$ as first discovered by Dimits [13] in a simple $\hat{s}\text{-}\alpha$ geometry. In all three simulations, the zonal flow activity is quite substantial – as has been known for a long time from tokamak studies of adiabatic ITG turbulence. The assumption of electron adiabaticity seems to strongly enhance zonal flows, such that it will be interesting to see their effect in more realistic simulations with nonadiabatic electrons. Such studies – which are left for future work – will require a lot of computational resources, however, mainly because the ragged structure of the geometric input data in the parallel direction leads to the requirement that at least some 100 parallel grid points are to be used (with associated small time steps).

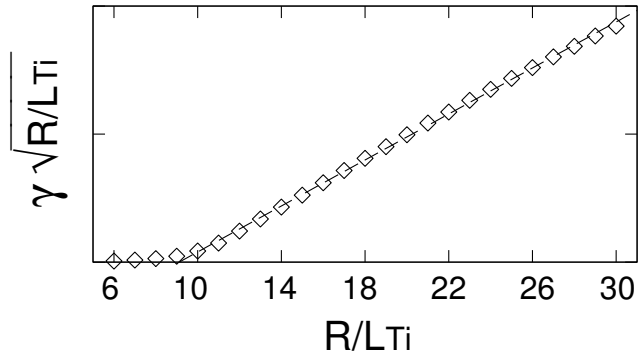


Figure 7: The rescaled linear growth rate of the toroidal ITG mode is well described by the fit curve $\gamma \sqrt{R/L_{T_i}} \propto [R/L_{T_i} - (R/L_{T_i})_{\text{crit}}]$ (dashed line) which provides the effective threshold: $(R/L_{T_i})_{\text{crit}} \approx 9$.

Linear parameter scans in which we changed the density gradients and the temperature ratio revealed that adiabatic ITG turbulence in Wendelstein 7-X behaves a lot like that in a usual tokamak.[14] Interestingly, in the nonadiabatic electron case, significant differences occur. For example, an ITG mode with full electron dynamics has a much smaller linear growth rate than its adiabatic counterpart as long as $R/L_{T_e} \ll R/L_{T_i}$. And even in the presence of a strong additional electron temperature gradient drive, i.e., for $R/L_{T_e} \sim R/L_{T_i}$, the increase in γ is only very moderate (of the order of a few 10%). This is in obvious contrast to tokamaks where trapped electrons are known to be able to boost the linear growth rate of ITG modes by factors of 2-3 or even more.

Substantial differences between the stellarator and tokamak configurations are also revealed through the investigation of TEMs. It has been mentioned before that for the Wendelstein 7-X configuration, the relative decoupling of regions with bad magnetic curvature and those with a large trapped fraction has a stabilizing effect on this mode. TEMs are thus expected to play a more moderate role in Wendelstein 7-X as in a tokamak. On the other hand, we find that their linear growth rates are by no means negligible, and that their critical gradients are relatively small. Thus, TEM turbulence can still play an important role in a device like Wendelstein 7-X. The decoupling mentioned above is not perfect and allows for significant TEM activity. This important point needs to be studied in more detail in the future.

5. Conclusions

In the present paper, we have described recent progress in the area of microturbulence research based on nonlinear gyrokinetic simulation and theory.

A systematic study of TEM turbulence revealed that its characteristics are very different from those of adiabatic ITG turbulence. In particular, nonlinear saturation is well described in the framework of a test mode approach in the spirit of renormalized perturbation theory, while zonal flows only play a subdominant role. This finding highlights the fact that our understanding of the underlying physical processes in plasma microturbulence is still quite fragmentary. Hence, more studies of various aspects of somewhat reduced systems are called for on the road towards reliable large-scale simulations.

Maybe surprisingly, it turned out that many nonlinear simulation results in the areas of TEM turbulence and particle pinch physics can be understood even quantitatively (!) in terms of carefully constructed quasilinear transport models. This raises the hope that – at least under certain conditions – key aspects of turbulent transport can be described reasonably well by such simplified descriptions. However, the limits of such attempts are obvious. It must therefore be kept in mind that transport models should always be firmly grounded on and tested against nonlinear gyrokinetics.

In conclusion, a synergistic interplay between experiment, modelling, simulation, and theory will remain the most promising path towards our ultimate goal, namely the thorough understanding, quantitative prediction, and control of turbulent transport in magnetic fusion devices.

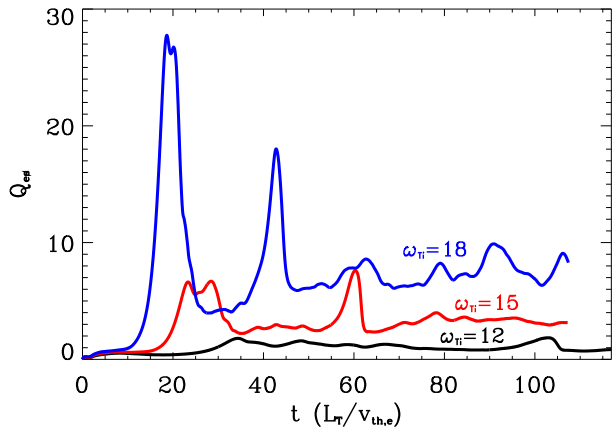


Figure 8: Nonlinear gyrokinetic simulation of adiabatic ITG turbulence in Wendelstein 7-X geometry: Normalized ion heat flux as a function of time for $\omega_i \equiv R/L_{T_i} \in \{12, 15, 18\}$.

References

- [1] F. Jenko et al., Phys. Plasmas **7**, 1904 (2000).
- [2] T. Dannert and F. Jenko, Phys. Plasmas **12**, 072309 (2005).
- [3] F. Ryter et al., Phys. Rev. Lett. **86**, 2325 (2001).
- [4] F. Ryter et al., Nucl. Fusion **43**, 1396 (2003).
- [5] C. Angioni et al.,
- [6] X. Garbet et al., Plasma Phys. Control. Fusion **46**, 1351 (2004).
- [7] R.E. Waltz et al., Phys. Plasmas **4**, 2482 (1997).
- [8] M.B. Isichenko et al., Phys. Rev. Lett. **74**, 4436 (1995).
- [9] F. Jenko et al., Plasma Phys. Control. Fusion **47**, B195 (2005).
- [10] G. Grieger et al., *Plasma Physics and Controlled Nuclear Fusion Research 1990* (International Atomic Energy Agency, Vienna, 1991), Vol. 3, p. 525.
- [11] P. Xanthopoulos and F. Jenko, Phys. Plasmas **13**, 092301 (2006).
- [12] M.A. Beer, Ph.D. Thesis, Princeton (1995).
- [13] A.M. Dimits et al., Phys. Plasmas **7**, 969 (2000).
- [14] P. Xanthopoulos and F. Jenko, submitted to Phys. Plasmas.